ENHANCEMENT OF DUAL PHASE PULSATING HEAT PIPES USING HYBRID FERRITIC NANOFLUID UNDER ACTIVE MAGNETIC FIELD

MD.AKIB KHAN
STUDENT ID:1510168

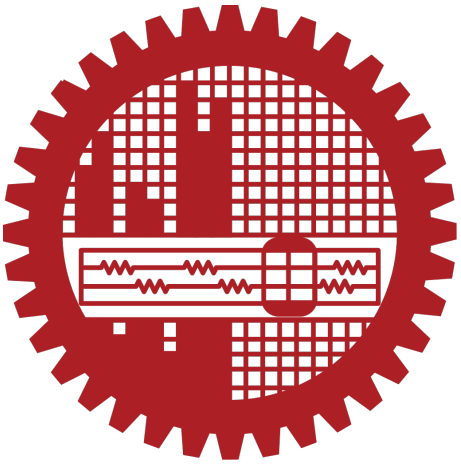

ME-400 : Project and Thesis

Bachelor of Science (B.Sc.)
Mechanical Engineering
Bangladesh University of Engineering and Technology(BUET)

February 2021 – Final Thesis

SUPERVISOR:
Dr.AKM Monjur Morshed
Professor
Department of Mechanical Engineering,
BUET

PUBLISHING DATE:
February 2021

Md.Akib Khan
Student Id:1510168; *Enhancement of Dual Phase Pulsating Heat Pipes using Hybrid Ferritic Nanofluid under Active Magnetic Field,* ME-400 : Project and Thesis,

COLOPHON

This document was typeset using the typographical look-and-feel `classicthesis` developed by André Miede. The style was inspired by Robert Bringhurst's seminal book on typography "*The Elements of Typographic Style*".
The monospace typesetting is done using Vera Mono by Jim Lyles and some spacing is done by Robert Slimbach's Minion Pro.
The template has been extensively modified and personalized by the author under creative common license and is not intended for commercial use.Distribution or unauthorized use of the current version is strictly prohibited.

DECLARATION

The thesis entitled "Enhancement of Dual Phase Pulsating Heat Pipes using Hybrid Ferritic Nanofluid under Active Magnetic Field" has been performed under the supervision of Dr.AKM Monjur Morshed , Professor,Mechanical Engineering department, BUET , Dhaka for partial fulfillment of Bachelor of Science degree requirement.

The works presented in this thesis book are based on my own ideas and results presented in my own word , except where due reference is explicitly made.This thesis or any part of it has not been accepted for any other degree and is not concurrently being submitted to any candidature for any other degree or diploma.

Dhaka,Bangladesh, February 2021

Md.Akib Khan
Student Id:1510168

A good judgment is usually the result of experience
and experience is frequently the result of bad judgment,
but to learn from the experience of others requires those who have the experience
to share the knowledge with those who follow.

— Henry Petroski
To Engineer is Human ,
The Role of Failure in Success [32]

ACKNOWLEDGEMENTS

The author likes to express his deep gratitude to Dr.AKM Monjur Morshed Professor,Mechanical Engineering department, BUET , Dhaka for providing supervision,invaluable guidance and cordial mentorship during the completion of this work.

The author is also greatful to his family members for providing mental support in the time of need.

ABSTRACT

Despite being ergonomic heat exchanging devices , used extensively in electronics cooling due to their portability and fast response time , the performance of Heat Pipes are severely obstructed by limitations imposed by the working fluid's thermo-fluid properties.Heat transfer characteristics and cooling time of such a Pulsating Heat Pipe filled with Ferrofluid under magnetic field has been investigated in this computational study using CFD-CHT simulations based on Finite Volume Method implemented by AnSys FLUENT with the MHD module addon to transcend the aforementioned limitations.Heat transfer and cooling time under realistic thermal loading condition was analyzed with and without presence of magnetic field and the results were compared with that of conventional water loaded ones.Increased heat transfer and faster evaporation onset was observed with ferrofluid and the performance was much more improved when magnetic excitation was applied.Significant reduction in marginal cooling time compared to regular heat pipes was indicated by the simulation results pushing the boundaries set by material properties and enhancing the overall heat pipe performance.

CONTENTS

LIST OF FIGURES

LIST OF TABLES

LISTINGS

LIST OF SYMBOLS

k_{eff}	effective thermal conductivity
B	applied total magnetic flux intensity
T	average absolute temperature of fluid
ϕ	volume concentration of nanoparticle in the ferrofluid
U	average flow velocity
Δt	timestep size
Δx	characteristic length of cell
γ_w	surface tension of water
T_c	critical temperature of fluid
ρ	density
$_{nf}$	nanofluid
$_{np}$	nanoparticle
$_{bf}$	bulk fluid
C_p	specific heat capacity
μ	dynamic viscosity
k	thermal conductivity
n	shape factor
P	perimeter of nanoparticle boundary
A	surface area of nanoparticle
σ	surface tension of nanofluid
L_v	latent heat of vaporization
T_{bp}	boiling point
h_0	standard state intensive enthalpy
s_0	standard state intensive entropy
Λ	electrical conductance
κ	magnetic susceptibility
R	loop bend radius
r	cross sectional radius
δ	wall thickness
l	adiabatic overrun
A_s	surface area
q_{evap}	evaporator heat flux
Q	volumetric flow rate
D	fan size
σ_b	fan solidity
A_f	flow area
V	flow velocity

Pr	Prandtl Number
Re_x	Reynold's Number
Nu_x	Nusselt Number
h_{prongs}	convection coefficient for fin prongs
a	fin length
b	prong height
c	fin width
θ	fin pitch
A_{fin}	fin effective area
h_{floor}	convection coefficient for fin floor
Q_{cond}	cooling load at condenser
q_{cond}	condenser heat flux
T_f	average fin surface temperature
T_∞	surrounding temperature
$\vec{\nabla}$	vector differential operator
$\widetilde{\mu}$	absolute magnetic permeability
$P(x)$	pressure field distribution

ACRONYMS

PHP Pulsating Heat Pipe

FVM Finite Volume Method

CFD Computational Fluid Dynamics

CHT Computational Heat Transfer

MHD Magneto Hydro Dynamics

CNT Carbon Nano Tube

MHT Magneto Hydro Thermal

WCS World Coordinate System

CFL Courant-Friedrich-Levy

Re Reynold's Number

Nu Nusselt Number

VOF Volume of Fluid

RNG Recurrent Normalization Group

SCM Scheme Customized Material

UDF User Defined Function

UDS User defined Scalar

CPU Central Processing Unit

TDP Thermal Design Power

TUI Text User Interface

PISO Pressure Implicit with Splitting Operation

SIMPLEC Semi Implicit Method for Pressure Linked Equation with Consistency

SIMPLE Semi Implicit Method for Pressure Linked Equation

CFM Cubic Feet per Minute

SI Systema Internationale

GUI Graphical User Interface

CSV Comma Separated Values

PWM Pulse Width Modulation

Part I

INTRODUCTION

A brief discussion on the motivation for the current work,literature review of the works leading up to it and short acquaintance with the fundamental parameters and equations used in the mathematical modelling process.

1 MOTIVATION

1.1 STIMULUS FOR THIS THESIS WORK

Pulsating heat pipes are passive heat transfer devices that cool objects, mostly hot electronic components that require fast cooling under fluctuating load,by transferring the heat to a working fluid by convective process , which can be both single or multiphase, in a pulsating manner.These devices are essential to get the maximum effectiveness of electronic devices as the performance of electronic components decline exponentially with incremental heat accumulation.Development of a high performance heat pipe will improve usability of electronic devices.But unfortunately there is a limit to this performance enhancement due to low thermal conductivity of available working fluids.This limit however can be transcended if nanofluids are utilized.

Nanofluids are colloidal suspension of nanoscale particulates or structures(nanotubes,nanosheets or nanofibers) in a base fluid.Due to the presence of condensed nanomaterials,thermophysical properties of the base fluid such as convective heat transfer coefficient,diffusivity, specific heat and thermal conductivity of the overall coloidal system increases significantly.This enhanced characteristics makes them an ideal choice as working fluid for many heat transfer equipment including heat pipe. Using nanofluids as working fluid in heat pipes ,independent of the operation type, increment in the performance beyond the capability of ordinary fluid can be achieved.Although there are still problems.Most prominent problem is that the fluid flow faces high drag due to enhanced vortex creation by the moving nanoparticles.Also agglomeration of nanoparticles during evaporation results in segregation of the fluid mix.

To push the limits furthermore magnetic effects could be used. If the nanoparticles suspended in the nanofluid are magnetically responsive, their motion can be controlled via application of active magnetic field.Schliomis et al.[39] demonstrated that such a setup can achieve negative viscosity , that is instead of dragging the flow down the continual shearing of the fluid boosts the flow. This increased mobility adds up to the overall heat transfer coefficient by increasing the associated Reynold's number and the thermal performance is improved much more by thermal conductivity improvement due to microscale induction chaining as reported by Shahsavar et al.[36].

Multiphase application of nanofluids creates some problematic issues regarding stability of the nanofluid.For example deposition of

nanoparticles occur at corners and wicked structure can't be used as it interferes with the flow streamline.Also because of the magnetic field assembly the setup needs to be shielded from other components for which magnetic field interference could be hazardous.
In recent years the idea of using nanofluids for heat pipe performance enhancement has been investigated by many researchers.The idea of magnetic field coupling is something that deserves attention as it could be the next big leap in creating next generation heat pipes.This is the major driving potential for the current work.

1.2 SCOPE OF THE CURRENT WORK

1.2.1 *Applicability*

The present work aims to investigate the effects of magnetic field on naofluid heat transfer behavior. This objective is accomplished by considering a pulsating heat pipe of realistic dimension , loading it with thermal load based on practical in-situ data and observation of the cooling behavior of the heat-pipe under different working fluid conditions and operational circumstances.
The study is purely computational in nature and hence acts only as a model to gain insight about the test conditions.Analysis is done based on Finite Volume Method (FVM) approach of Computational Fluid Dynamics (CFD) with Computational Heat Transfer (CHT) and Magneto Hydro Dynamics (MHD) considerations.
The model used and the subjected boundary conditions are kept invariant throughout the simulation.Under this invariant setup performance of conventional working fluid(i. e.water) , naofluid in magnetically uncoupled state and nanofluid in magnetically coupled state are simulated.Comparison of these simulation based results are done by visualizing the raw and non-dimensional data regarding thermal performance of the differing conditions.The similarity in setup and non-dimensionalization makes the solution datasets easily comparable.

1.2.2 *Organization of the Thesis*

The first part of the thesis contains introduction to the subject matter by presenting chapters on motivation for the work , literature review of related works in the field and basic theory associated with the analysis and methodology.
The second part presents the research methodology in detail where the complete simulation and result preparation process is outlined with full technical description to illustrate the author's complete procedural journey in arriving at the conclusions.This portion is sepa-

rated in 5 distinct chapters on preprocessing,mesh validation ,simulation setup , calculation procedure and postprocessing respectively.
The third and final part contains 3 chapters to exhibit the conclusion of work.The chapters are on results, discussion and future recommendations based on the author's remarks.
First part of the thesis can be skipped without any loss of continuity by the reader if the reader is familiar with the subject matter.The second part is only needed in case the reader is interested in reproducing the result or understanding the computational schemes.The third part is the core part and Chapter 9 contains all the results in a compact manner which conveys the fundamental achievement from this work.

2

LITERATURE REVIEW

Pulsating heat pipes were introduced by Akachi[18] as an alternative to capillary ones and these showed much more uniform heat transfer over the whole fluid domain rather than localized heat fluxes present in conventional ones.Since it's introduction Pulsating Heat Pipe (PHP)s have found widespread use and have acted as a very good alternative to regular heat pipes.
The introduction of nanofluid in heat pipes began soon after Choi and Eastman[9] reported it's enhanced thermal properties.Kang et al[25] presents a comprehensive summary of such attempts and presents graphical comparison among various test cases.
At this point a focus shift on engineering the nanofluids according to need found immense attention.Most of these demonstrated effect of size , fabrication method and surface characteristics of naonoparticles to innovate new blends with enhanced thermal performance.Chen et al.[7] , Yang et al.[49] ,Hwang et al.[24] and Tang et al.[42] presented many such results.Although this results were important to understand improvement schemes for nanofluids , such ex-situ treatment was not beneficial for understanding heat pipe or other device application behavior of the nanofluid.
More recent works focused directly on nanofluid loaded heat pipe investigations.Tanshen et al.[43] investigated thermal resistance reduction in heat pipes when various water based nanofluids are used separately.Goshayeshi et al.[17] demonstrated particle size effect on thermal resistance of heat-pipes.Mehrali et al.[29], Nazari et al.[33] and Xie et al.[48]presented findings on consequences of various types of nanoparticle usage.Sheikholeslami et al.[37] presented argument from energetics point of view in favor of nanofluids.
During the same time as the previously mentioned results , Hordy et al.[22] and Anushree et al.[8] worked on stability of nanofluids in heat pipes and showed a narrow range of stability in multiphase application.This presented a crucial problem that required resolvance before successful implementation of nanofluid in heat-pipes.
Ghofrani et al.[16] reported enhanced thermal behavior of ferrofluids flowing over flat plate when operating under influence of alternating magnetic field.This introduced the possibility of magnetohydrodynamic effect to be used to overcome non-magnetic nanofluid limitations.
The major hindrance now was the high viscosity and less fluidity of ferrofluids in constricted channels.In very recent times this problem has been partly mitigated by engineering ferrofluids with hybrid par-

ticles and using essential oils with additives as bulk fluid as reported by Fakour et al.[14] and Schliomis et al.[39].
This improved flow nature led to study of ferrofluid performance in constricted channels by Hussain et al.[23] and Mousavi et al.[31].Recent performance of this works strongly suggest application of ferrofluid under magnetic field in heat pipes would improve performance.

3

HEAT PIPE AND FERROFLUID FUNDAMENTALS

3.1 HEAT PIPES

Heat pipes are small scale heat exchangers that essentially transport heat from a particular target location to another drop-off one where this carryover heat is eventually rejected.It can work in both single and multiphase modes.In single phase operation it relies solely on fluid convection for heat transfer which limits the thermal load bearing capacity and generally an external pump is required to maintain the convective stream. The multiphase ones absorb heat by utilizing phase change heat transfer.As the latent heat is generally very high the thermal load bearing capacity of this type is higher than the former one.Furthermore the gaseous phase can maintain fast enough convective stream due to low inertia.This makes multiphase heat pipes the popular choice.
Multiphase heat pipes can be broadly classified into two categories.

1. Capillary Heat Pipes
2. Pulsating Heat Pipes

As the working fluid in multiphase heat pipes transform to gas during phase shift operation , reverting it back to the original phase is essential for cyclic operation of the device.This inverse phase shift is implemented by condensing the vapor in a condenser section which is generally air cooled using an induced draft fan.
Once the condensation is complete , the condensed fluid is to be returned to the heat removal or evaporator section.Capillary heat pipes accomplish this transportation by employing the capillary action of fluids.It is generally executed using a wick structure or etched nanoscale grooves on pipe-wall.
Pulsating heat pipes on the other hand accomplish the same task by utilizing pressure from the vapor itself.It uses pressure from a portion of vapor to move another portion of liquid.This makes pulsation of alternating liquid and vapor columns inside the pipe.These types carry less heat per cycle but take very low time per cycle which makes them ideal for real scenario where quick heat removal is needed.
Heat pipes assert their superiority by enabling quick heat transportation hence the faster the heat pickup rate at the evaporator would be ,the better the heat pipe would perform.But this pickup rate gets limited because of the thermal and fluidic limitations of the working fluid (i. e.viscosity ,thermal conductance).

3.2 NANOFLUIDS

Nanofluids are mix-blends of fluid with nanoparticle of some material (typically metal)added to them.The fluid acts as a regular convective heat transportation media while the inclusion of metallic nanoparticles enhance the overall thermal conductivity of the blend.This gives nanofluids enhanced thermal characteristics and makes them transcend the limitations of conventional working fluids.As nanofluids can provide faster heat pickup , they are the ideal candidates for next generation heat pipe application.
A major disadvantage of using nanofluids is that it can't be handled in a stable manner under phase change conditions.During evaporation of the bulk fluid , the nanoparticles subtended in the blend start to co-agulate.The process is further boosted by increment of temperature.This agglomeration of the particles create metallic deposit on the pipe-wall and because of the separation the fluid loses it's enhanced functionality.
Works of Anushree et al.[8] and Hordy et al.[22] has revealed this result based on computational study.

3.3 MAGNETOHYDRODYNAMIC EFFECTS

Magnetohydrodynamics is the study of hydrodynamic effects that can be directly attributed to and influenced by magnetic field parameters.Three major effects can be identified as crucial for our current purposes.They are-

1. The increased stream velocity in fluid due to magnetic force acting on nanoparticles with nonzero magnetic moments.This discretizeed particular movement creates a magnetohydrodynamic pressure[1] resulting in flow velocity increment.

2. Negative viscosity effect.In the presence of alternating magnetic field ferrofluids demonstrate negative viscosity resulting in drag attainment where viscous drag aids the flow.This eases the flow as overall wall shear is less than ordinary bulk fluid case.

3. Excitation of nanoparticles by magnetic field creates additional microvortex in the stream generating turbulent behavior throughout.This makes the flow much more active by increasing turbulent kinetic energy.

These magnetohydrodynamic effects help the fluid move in a much more vigorous way inside the heat pipe ensuring faster heated fluid transport.

1 see Appendix A for details

A power law model due to Shahsavar et al.[36] characterizes these effects.

$$\tau = c\gamma^n$$

The parameters c and γ are modelled as-

$$c = 24.769\left[\frac{1+608891214B-7813611.9B^2}{1-621740.5B-24961.852B^2}\right]\left[\frac{1+8.08\phi}{1+6.949\phi-0.083\phi^2}\right]$$

$$n = \left[\frac{1+0.063202B-0.000407B^2}{1+0.03038B-0.000212B^2}\right]\left[\frac{0.651+1.59(\phi-0.45)}{1+2.464(\phi-0.45)+0.05(\phi-0.45)^2}\right]$$

where
- B applied total magnetic flux intensity
- ϕ volume concentration of nanoparticle in the ferrofluid

Although these results were specifically for Carbon Nano Tube (CNT) based ferrofluids , similar result can be expected in all ferrofluids.

3.4 MAGNETOTHERMAL EFFECTS

Thermal property of the fluid is influenced by magnetic field in mainly two ways.

1. Hot ferrofluid under magnetic field undergoes a complex bulk reasssortment which generates a tendency to flow in the fluid.This is called thermomagnetic pumping and this effect makes heat pipe response time shorter.
2. Magnetic field realligns the magnetcally coupled nanoparticles forming temporary diffusion chains in the ferrofluidat different places.This increases the overall heat diffusion which in effect enhances the overall thermal conductivity.

The thermal conductivity variation due to magnetic field and temperature can be modeled by the correlation proposed by Shahsavar et al.[36].

$$k_{eff} = (10^{-10}B^4 - 2\times10^{-7}B^3 + 7\times10^{-5}B^2 - 0.0096B + 0.88)\\ (0.0006T^2 - 0.046T + 1.77)$$

where
- k_{eff} effective thermal conductivity
- B applied total magnetic flux intensity
- T average absolute temperature of fluid

This model represents enhanced Magneto Hydro Thermal (MHT) effects of the ferrofluid under magnetic field and the model parameters have been verified numerically.

Part II

RESEARCH METHODOLOGY

Detailed discussion on the complete methodology including model making,mesh creation , simulation setup ,calculation procedure and post processing schemes with necessary mathematical analysis.

4

PREPROCESSING

4.1 PHP MODEL

To simulate effect of fluid property variation only , the same heat pipe model is used in all simulations. The model dimensions are chosen based on Antec A400 heat pipe[1] as it is a popular model fabricated using the most recent design for heat pipes.Modifications have been made to the aforementioned dimension to adapt it as a PHP and meet ferrofluid application conditions.The final model dimensions are presented in the sketch below.

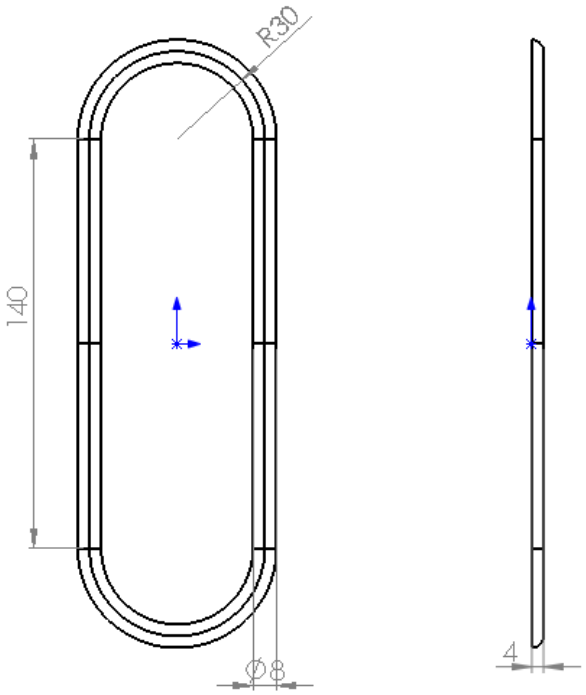

Figure 1: Orthographic projection sketch of model

As this model is based on practical design , the simulation results are expected to be realistic.
The model for simulation is made using *SolidWorks*® and the 3d model is then loaded in *DesignModeler*® where it is unfreezed , to permit free motion of fluid throughout the whole domain , and then segmented into distinct sections for evaporator , adiabatic conductor and condenser by using split operation with reference planes.The World Coordinate System (WCS) was set up with the geometric centroid as origin and *y-axis* pointing from evaporator to condenser.

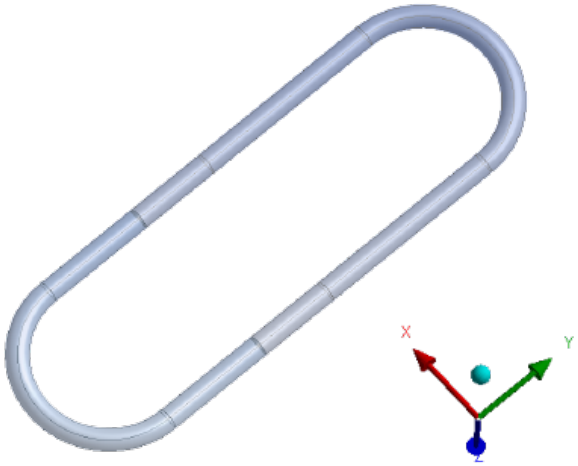

Figure 2: 3D model with WCS orientation

The model was made as a symmetric half-section to observational provision to the central plane for monitoring the thermal and phase transition progression during the simulation.Contrary to most regular PHPs only a single loop is considered to reduce computational complexity.The outer walls are not modeled and are indicated only during the setup phase in Chapter 6.

4.2 SEGMENTATION DATA

4.2.1 *Thermal Zone*

Like all heat pipes three distinct zones for evaporator , adiabatic conductor and condenser have been created.The zone markup is done using the *Named Selection* feature .

NAME OF ZONE	LENGTH SPAN	RELATIVE PROPORTION
Evaporator	30 mm	15%
Adiabatic Conductor	70 mm	35%
Condenser	100 mm	50%
Total	200 mm	100%

Table 1: Zone Proportions in the Model

The condenser portion is made significantly larger than evaporator to facilitate condensation as pointed out by Silverstein[40].

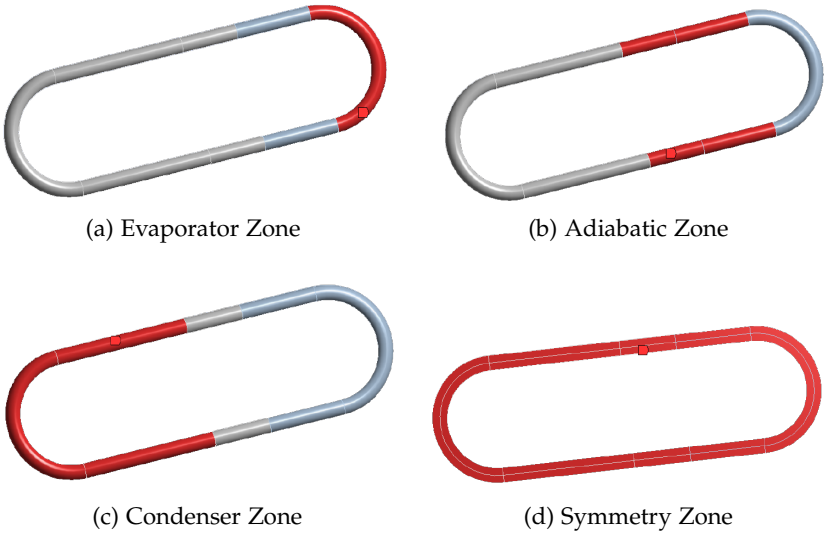

(a) Evaporator Zone (b) Adiabatic Zone

(c) Condenser Zone (d) Symmetry Zone

Figure 3: Zone Markup of the Model

An additional zone is marked up as symmetry zone to facilitate application of boundary condition later during setup phase in Chapter 6.

4.2.2 *Filling Ratio*

Filling ratio is crucial to heat pipe performance.as reported by Thrayil et al.[45] and Shi et al.[38] too high filling ratio hinders completion of proper condensation and too low filling ratio creates accelerated void life which stalls the cycle.
In accordance with these results an optimum fill ratio of 35% is chosen for the present simulation.The air over the working fluid is set up in vacuum pressure levels to permit low temperature vaporization and match the thermal loading scenario.

4.3 MESH GENERATION

The mesh for this problem has high dependency on cell size rather than cell shape.As the simulation is performed considering phase transition and mass transfer , requirements on *Courant-Friedrich-Levy (CFL) Number* are to be satisfied to ensure solution convergence and stability.The *CFL Number* is given by-

$$\mathrm{CFL} = \frac{U\Delta t}{\Delta x}$$

where
- U average flow velocity
- Δt timestep size
- Δx characteristic length of cell

Using this equation and considering optimum timesteps investigated in the works of Ma et al.[27] a cell size of 1.5976×10^{-5} order is chosen.The size couldn't be reduced furthermore due to unavailability of sufficient computational power.

Figure 4: Meshing used for the simulation

Shape of the cells are tetrahedral with adaptive sizing throughout.The relevance center is set at fine mesh conditions and inflation adjustment has been done.Some cells in the symmetry face have been base flattened to facilitate application of symmetry boundary condition.

5 MESH VALIDATION

5.1 MESH CASES

To validate the generated mesh , two different meshing constructs are used to generate two different meshing setups with distinct cell sizes.These test meshes are run through simulation under similar test condition where the test condition is set up using a results that have already been studied and verified prior to this research.

MESHING PARAMETER	MESH-1	MESH-2
Nodes	8876	9065
Elements	5923	6176
Minimum Cell Size	3.1952×10^{-5}	1.5976×10^{-5}

Table 2: Mesh data for test meshes

The number of element in the domain is varied by changing mesh characteristic length parameter available in *MeshModeler*®.Inflation adjustment ,relevance center and smoothing options are kept unchanged to maintain similar mesh distribution.

5.2 MESH INDEPENDENCE TEST

Ideally the non-dimensional parameter response should be invariant under different extensive dimensions as long as the requirements for principle of similitude are satisfied.This is due to the fact that non-dimensional parameters are of intensive nature and only depend on the systems basic nature.
As the two types of meshes generated fulfill all similitude requirements , a non-dimensional response analysis should yield nearly invariant result in both setups independent of the mesh construct.There will be certain deviations due to the approximate nature of the method employed in the study.These approximate computational methods rely on some parameters that do change with respect to cell size which in turns produce slight discrepancy.
To test mesh independence the two meshes are set up with similar boundary conditions and simulation is run with few number of iteration but with small step-size.The solution data obtained from

the simulation is then used to generate Nusselt Number (Nu) versus Reynold's Number (Re) graph representing heat transfer characteristics in the two cases.Data for these parameters are taken at the evaporator section as the significant portion of heat transfer occurs in this section.The two curves are plotted against each other and similarity trend is observed.

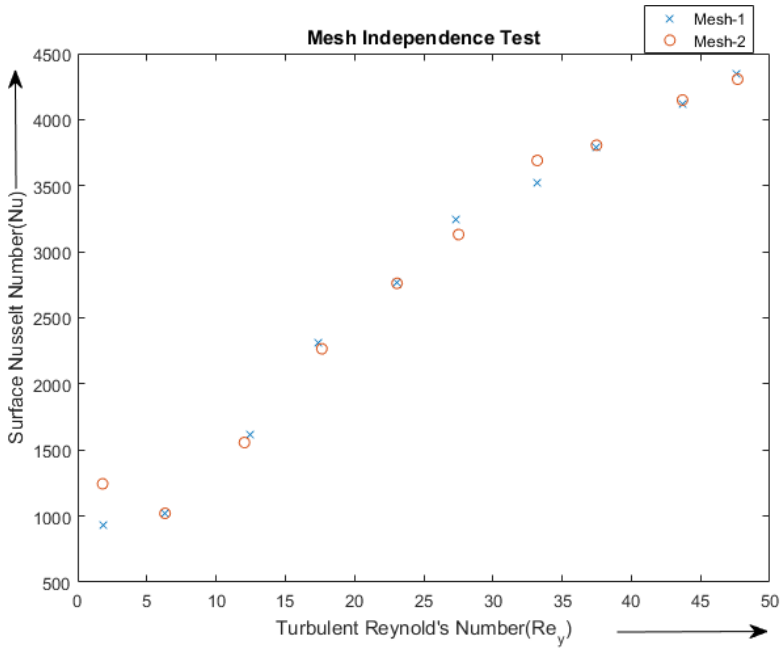

Figure 5: Nu vs. Re plot in evaporator section for two distinct mesh constructs

The curves show near perfect match which provides judgment in favor of mesh independence.The deviation between the two data is maximum at low Re . This is because at low Re the fluid velocity is low which makes computation of velocity field and hence the overall convective field erraneous due to high truncation error.
Apart from the mutual similarity between the two test meshes , the results are also in agreement with the works of Taler[41] and Hong[21] which provide empirical correlations producing results of similar order.

6 SIMULATION SETUP

The PHP model is loaded in *Fluent®* , after proper meshing and zone markup , for simulation.Simulation mode is chosen to be transient as dynamic response of the system and transition onsets are sought after in this study.As *y-axis* was chosen along the heat pipe from evaporator to condenser , gravitational field is activated along negative *y-axis* to simulate gravity opposed flow condition. This is done to test the performance of the heat pipe under worst case scenario which derates the true performance allowing for a statistical margin of safety for the results.

6.1 MODELS

6.1.1 *Mixture Model*

As the heat-pipe is loaded in an air-over-liquid assembly and during operation vapor of the working fluid would be generated , a mixture model is needed to simulate the stream mixing along with heat and mass transfers.The Volume of Fluid (VOF) model is used to accomplish this objective.VOF model is chosen because-

A. it provides flexibility in adjusting the phase change parameters

B. it offers simpler control of species concentration in the mixture

Three Eulerian phases are assigned as VOF mixture species which are set as primary and secondary phases.Air is set as the primary species to make volume fraction calculations simpler and the two secondary phases are assigned by liquid and vapor phases of the working fluid.
Under the VOF model two types of phase interaction are set-up.

- `Mass Transfer Modes:`
  - evaporation-condensation type of mass transfer from working fluid's liquid phase to vapor phase is set as the only mass transfer mechanism.Lee model is used to model the process and saturation temperature of the fluid is set as 333.15 K(60°C) to enable vaporization at the working temperature.The condensation frequency is set higher than the evaporation frequency to aid the slow condensation process.

- `Surface Tension:`
  - surface tension between working fluid and air is assumed to be constant
  - for vapor-air surface tension molecular dynamic Boltzmann model is used and value is extrapolated upto vapor region
  - the liquid-vapor surface tension is modeled using IPAWS[46] equation for steam.

$$\gamma_w = 235.8\left(1-\frac{T}{T_c}\right)^{1.256}\left[1-0.625\left(1-\frac{T}{T_c}\right)\right]\times 10^{-3}$$

where γ_w surface tension of water; T average absolute temperature Proportional; T_c critical temperature of fluid

variation of water-steam pair based on this equation is used as a guideline for computing liquid-vapor pair surface tension.

  - wall adhesion effects have been considered

Following the procedures stated so far , the VOF model is adjusted to be as realistic as possible.

6.1.2 *Viscosity Model*

Due to low viscosity of the naturally convected fluid stream , working fluid in heat-pipes can be reliably modeled using the laminar model.But as the present work aims to observe viscous variations with significance , the $k-\epsilon$ model is used.
This two equation model solves two additional parameters , namely turbulent kinetic energy(k) and energy dissipation rate(ϵ).Under model options realizable scheme is used contrary to the popular Recurrent Normalization Group (RNG) scheme to make the model parameters adapt based on flow conditions.
Enhanced wall treatment and curvature correction is also activated to account for any additional wall shear variations due to external magnetic field.

6.2 MATERIAL SETUP

6.2.1 *Material Property*

The nanofluid used for the current work is modeled closely contrasting with APG E-32 black-brown synthetic ferrofluid by Ferrotec[50] because of it's excellent thermal properties. The fluid is then engineered based on popular available choices to meet viscosity requirements.The final fluid considered is a mix of ferrite nanoparticles with

a blend of acetone and essential oil.
Properties of the nanofluid are calculated based on proven and validated correlations.The following equations have been used-

Mass Balance :

$$\rho_{nf} = \phi\rho_{np} + (1-\phi)\rho_{bf}$$

where
- ρ density
- ϕ volume fraction
- $_{nf}$ nanofluid
- $_{np}$ nanoparticle
- $_{bf}$ bulk fluid

Weighted Energy Balance(Eastman et al.[12]):

$$C_{nf} = \frac{\phi\rho_{np}(C_p)_{np} + (1-\phi)\rho_{bf}(C_p)_{bf}}{\rho_{nf}}$$

where
- C_p specific heat capacity

Tuned Vicosity Model(Maiga et al.[28]):

$$\mu_{nf} = \mu_{bf}(1 - 0.19\phi + 3.6\phi^2)$$

where
- μ dynamic viscosity

Hamilton-Crosser Model[19]:

$$k_{nf} = k_{bf}\frac{k_{np} + (n-1)k_{bf} - (n-1)(k_{bf} + k_{np})\phi}{k_{np} + (n-1)k_{bf} + (k_{bf} + k_{np})\phi}$$

$$n = \frac{P}{\sqrt{A}}$$

where
- k thermal conductivity
- n shape factor
- P perimeter of nanoparticle boundary
- A surface area of nanoparticle

The property data for oil in the blend is taken from Bejan[5] and Faghri[13] , acetone data is collected from NIST[3] and pubchem[2] database and ferrite data is collected from Ferrotec[50] website.Typical shape factor value is taken from Tora et al.[47]
For MHD analysis additional electromagnetic properties are needed.The electrical conductance data is due to Chang et al.[6] , magnetic permeability is taken from DOE[10] catalog and magnetic saturation is from Ferrotec[50] website.

6.2.2 *Material Entry*

As the nanofluid used in the simulation is custom engineered it's property data is to be manually included in *Fluent*® database , preferably in a user defined database , before this material can be assigned to phases.This is done using a database entry scheme-code passed as a Scheme Customized Material (SCM) file.

Listing 1: SCM Code

```
((nanofluid
fluid
(chemical-formula. ferrofluid-OOEO)
(density (constant. 1168))
(specific-heat (constant. 1524))
(thermal-conductivity (constant. 0.1548))
(viscosity (constant. 0.00025))
(molecular-weight (constant. 58.0498))
(reference-temperature (constant. 298))
(formation-enthalpy (constant. -2.49e+08))
(formation-entropy (constant. 295350))
(latent-heat (constant. 501033.1))
)
(nanofluid-vap
fluid
(chemical-formula. ferrofluid-OOEO-vap)
(density (constant. 0.6465))
(specific-heat (constant. 1168))
(thermal-conductivity (constant. 0.016))
(viscosity (constant. 2.5e-06))
(molecular-weight (constant. 58.0498))
(reference-temperature (constant. 298))
(formation-enthalpy (constant. -2.03e+08))
(formation-entropy (constant. 1800000))
))
```

Once the material is registered it can be accessed from the database.To account for magnetic field and temperature influence on thermal con-

ductivity , a User Defined Function (UDF) is included in the environment which is tagged to the material during assignment.

Listing 2: UDF Code

```
#include "udf.h"

DEFINE_PROPERTY(thermal_conductivity,c,t)
{
        real keff;
        real b=NV_MAG(x[1]);
        real temp=C_T(c,t);
        keff=(pow(10,-10)*pow(b,4.)-2*pow(10,-7)*pow(b
            ,3.)+7*pow(10,-5)*b.*b-0.0096*b).*(0.0006*pow
            (T,2.)-0.046*T+1.77);
        return keff;
}
```

Finally two User defined Scalar (UDS) are added to the material panel to account for magnetic susceptibility and coupling , which are calculated during each iteration.

6.3 CONDITIONS

6.3.1 *Boundary Conditions*

The heat-pipe has four distinct surface zones , as marked up in Chapter 4.All of these surfaces must be assigned proper boundary conditions before solution process is started.The boundaries here are finite surfaces and can be set with isothermal or isoflux conditions instead of a field function without loss of generality.To simulate realistic situation , isoflux conditions are used

- `Evaporator:`
  The evaporator is set to receive apositive heat flux of value 5572 W/m^2 as calculated in Chapter 7.A continuous heat flux would make the temperature variation rate slower and hence would take large number of time-steps to observe.To eradicate this problem a pulse of heat flux is applied for a finite amount of time which acts as the thermal load.The pulse of flux is set as a profile function written in Scheme-programming which is passed via a Prof file.

Listing 3: Prof Code

```
((varHeatFlux transient 5 0)
(time
0
0.0006
0.0012
0.0018
0.0024
)
(hf
5572
5570
5568
5566
5564
))
```

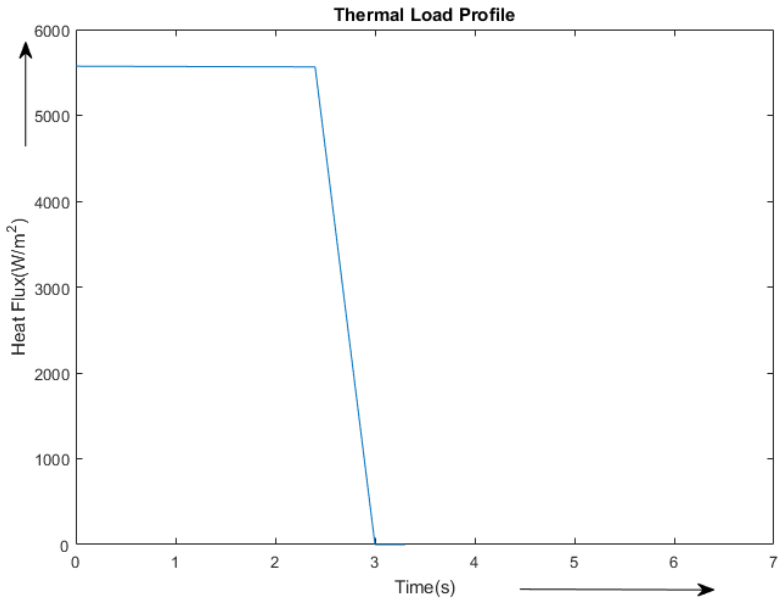

Figure 6: Pulse type isoflux thermal loading

- `Adiabatic Conductor:`
  As the name suggests this part is kept adiabatic to stop stray heat fluxes and reduce unwanted flow crossings.Isoflux condition with zero heat flux are assigned here.

- `Condenser:` This part does the heat rejection to initiate condensation in the void flashed at evaporator.The isoflux condition is only an approximation here as fin cooling with ID fan always

has some intrinsic variability.As calculated in Chapter 7 , the flux value is set to be 342 W/m^2 with a negative sign to indicate rejection.

- `Symmetry:`
  The symmetry zone is marked-up at the central plane hence for axisymmetric operation a thermal symmetry is expected at this location.This is set by changing the type of boundary condition to symmetry type.

Also wall thickness of 0.001 m is inserted in all the surfaces to account for wall thermal resistance and wall material is set as copper.

6.3.2 *Initial Conditions*

As VOF model is used to simulate the dynamics , volume fraction in all domains must be satisfied at the starting time which will act as essential initial conditions for the forward time integration process.Initial temperature in the domains can also be set but by default they are automatically set to operating temperature and hence can be skipped.
The complete 3D domain is essentially separated in two phases at the beginning , the working fluid liquid phase and air phase.Working fluid vapor would be produced once thermal loading is activated and therefore at the beginning the vapor should be absent in all domains.The boundary of the two phases are already created via splitting operation as mentioned in Chapter 4.
The initial volume fractions expressed as proper percentages are then set by using the patch option once solution initialization is done.The initialization is done using *hybrid initialization* scheme to keep an initial gradient present in the parameter fields due to the presence of different seed values at the cells which reduces number of iterations.

NAME OF DOMAIN	AIR VF	LIQUID VF	VAPOR VF
Working Fluid Domain	0	1	0
Void Domain	1	0	0

Table 3: Initial volume fractions patched at domains

6.3.3 *Operating Conditions*

The heat-pipe is employed for electronics cooling(e. g.Central Processing Unit (CPU) cooling) in practice.The safe CPU temperature as men-

tioned by Brent[35] is around 50°C and common Thermal Design Power (TDP) as reported by Ixtlabs[44] projects the peak value in running condition to be in the range of 70 °C ~150 °C , where the upper limit is the worst case scenario according to Li[26].
To provide proper cooling in this wide range and reducing the temperature at asafe margin within reasonable time a flashing temperature of 60 °C is needed which has already been set-up in *Material Setup* section.
The saturation pressure at this flashing temperature is found using Antoine equation[15] given by -

$$P = 10^{A - \frac{B}{C+T}}$$

where the parameters A,B and C are found at Dortmund Data Bank[**dort**].
This saturation pressure and the marginal 50 °C temperature are set as the operating conditions for the setup.To allow more interpolating freedom , the Boussinesq parameter temperature is decreased by 20 °C from the operating temperature.

6.4 SOLUTION SETUP

To monitor vapor generation from the very beginning and observe complete cycle in multiple frames the time step is set in the order of 3×10^{-5} and the time-step iterations are run in groups of 1000.
During this progression data is saved at every 5 time-step and parameters saved in the case files are-

- Total Temperature
- Turbulent Viscosity
- Turbulent Re
- Surface Nu
- Heat Flux
- Volume Fraction of Phases
- Total Enthalpy

These are used in postprocessing stage as described in Chapter 8.
Apart from that filled contour plots of temperature and volume fraction of vapor are generated every time-step to generate and monitor solution parameter evolution with time.This is set in the calculation activities option.

6.5 MHD SETUP

To simulate the case where external magnetic field is activated an addon package with identifier MHD Module is needed.It's activated via command line input in the Text User Interface (TUI).

```
>>>define/models/addon-module
>>>1
```

Once enabled a model would be added to the list of models where external magnetic field,magnetic coupling of boundary surfaces and presence of any electrical potential can be specified with immense customization options.For the current work , only the evaporator and condenser sections are magnetically responsive to generate adequate thermomagnetic pumping preventing any backflow.Saturation magnetization was set to be 10 mT as specified in Ferrotec[50] database. Also magnetic permeance and electrical conductivity options are now available in the material property panel.These should be filled out correctly to ensure proper magnetic coupling is established.

7 CALCULATION

7.1 PROPERTY CALCULATION

Properties of the nanofluid are calculated using the equations mentioned in Chapter 6 and then passed to the material database via Listing 1.

PARAMETER	ASSIGNMENT
Bulk Fluid	Acetone and Buckwheat Oil Blend
Nanoparticle	LiTi Ferrite(α and γ variants)
Volume Fraction(%)	5.96
$\rho(kgm^{-3})$	1168
$\mu(Pa.s)$	0.00025
$C_p(kJkg^{-1}K^{-1})$	1.524
$k(Wm^{-1}K^{-1})$	0.1548
$\sigma(Nm^{-1})$	0.0212
$L_v(Jkg^{-1})$	501033.1
$T_{bp}(K)$	329.3
$h_0(Jkg^{-1})$	-2.49×10^8
$s_0(Jkg^{-1}K^{-1})$	295350
$\Lambda(Sm^{-1})$	2.5
κ	0.999465

Table 4: Properties of the model nanofluid

To account for dynamic property variation of the nanofluid during opertaion , some of these properties have been entered as piecewise polynomial functions in the material property panel ,where the polynomial parameters are taken from relevant sources mentioned in Chapter 6.

7.2 HEAT FLUX CALCULATION

7.2.1 *Evaporator Heat Flux*

Evaporator bend radius , $R = 30mm$
Pipe cross-section radius , $r = 4mm$
Wall thickness , $\delta = 1mm$
Adiabatic overrun , $l = 10mm$
Surface area ,

$$\begin{aligned} A_s &= (\pi R + 2l) \times \pi(2r + 2\delta) \times 10^{-6} \\ &= 3.59 \times 10^{-3} m^2 \end{aligned}$$

TDP=20 W
Applied thermal load ,

$$\begin{aligned} q_{evap} &= \frac{TDP}{A_s} \\ &= \underline{\underline{5572.27}} W m^{-2} \end{aligned}$$

7.2.2 *Condenser Heat Flux*

Fan data from antec[1]:

- Airflow , $Q = 77$ Cubic Feet per Minute (CFM)
- Fan size , $D = 6in$
- Fan solidity , $\sigma_b = 0.5$

Flow area of fan ,

$$A_f = \frac{1}{4}\pi\sigma_b D^2 \times 0.000645 = 9.12 \times 10^{-3} m^2$$

Air velocity ,

$$V = \frac{Q}{A_f} = 4.22 m s^{-1}$$

Air property data in operating condition(from Moran[30] in Systema Internationale (SI)):

- $\rho = 1.1945$
- $\mu = 1.83 \times 10^{-5}$
- $k = 0.0258$
- $Pr = 0.71512$

Appropriate fin data from Celsia[20] database,

Fin length(a)	120 mm
Prong height(b)	9.5 mm
Fin width(c)	38 mm
Fin pitch(θ)	1.38 mm
Fin area(A_{fin})	$0.036 m^2$

Reynold's Number , $Re_x = \frac{\rho V L}{\mu} = 1.65 \times 10^4$
Heat transfer coefficient in fin prongs due to Pitts & Sissom[11],

$$Nu_x = \frac{0.0288 Re_x^{0.8} Pr}{1 + 0.849 Re_x^{-0.1} \left\{(Pr - 1) + \ln\left(\frac{5Pr+1}{6}\right)\right\}}$$
$$\implies Nu_x = 59.33$$
$$\implies h_{prongs} = 25.5 W m^{-2} K^{-1}$$

Heat transfer coefficient in fin floor due to Agarwal et al.[34] ,

$$h_{floor} = 0.0872\theta V^{0.9}(2.47 - \frac{2.55}{\theta^{0.4}}) + 4.31 = 4.312 W m^{-2} K^{-1}$$

Total fin heat transfer,

$$\begin{aligned} Q_{cond} &= b \cdot c \cdot h_{prongs} \left(\frac{a}{\theta} + 1\right)(T_f - T_\infty) + a \cdot c \cdot h_{floor}(T_f - T_\infty) \\ &= 12.3 W \\ q_{cond} &= \frac{Q_{cond}}{A_{fin}} \\ &= \underline{\underline{342}} W m^{-2} \end{aligned}$$

7.3 SOLUTION METHOD

Although Pressure Implicit with Splitting Operation (PISO) is the most popular solution method for transient problem , it is not suitable for handling MHD module due to accelerated divergence produced by splitting action on the fields.
Semi Implicit Method for Pressure Linked Equation (SIMPLE) could be used but it produces inconsistent and unstable result when energy field faces significant transition rate.This problem is eliminated in Semi Implicit Method for Pressure Linked Equation with Consistency (SIMPLEC) method , making it the ideal choice for the present problem.

Before solver is run proper time-step is to be selected to ensure convergence.Although the CFL number gives aguideline , this selection is mostly trial and error.Also the under relaxation factor for energy parameter should be decreased to adapt with the large variations in energy during the thermal loading application period.It is generally set as unity but should be tweaked until convergence is found.For the current work a value of 0.7 did the job.This is set under solution control submenu.
To ensure high precision three steps are taken.

- residual tolerance should be set as at least one tenth order of cell size
- residual normalization should be enabled to prevent overshoot
- residual re-feed mechanism should be activated to let the solution process adapt based on produced residuals

Before running it should be checked that proper initialization and patching have been done and iterations should be run in successive groups rather than all-at-once to monitor and change free variables if necessary.

8

POST PROCESSING

The setup described in earlier chapters is done once and the ready-to-simulate model is linked to distinct solution environment via branching.

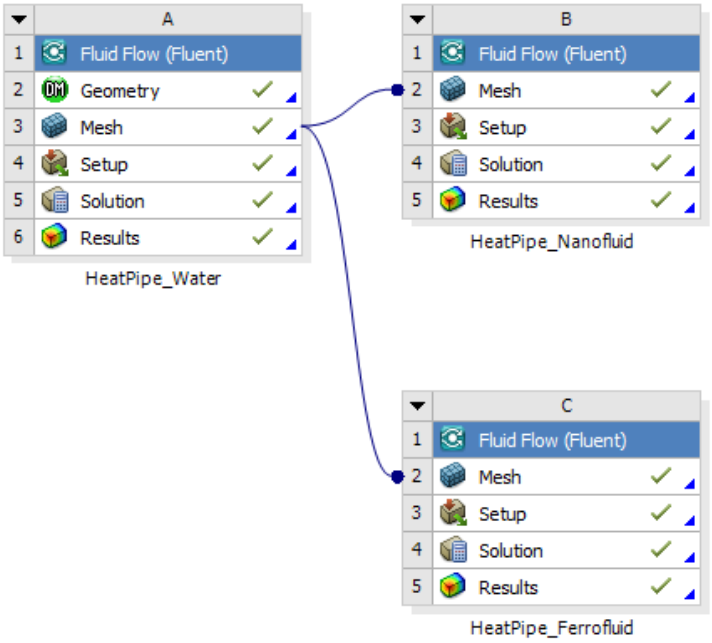

Figure 7: Project Map

8.1 CFD POST

The initial post processing is done in *CFD Post*® .Here the parameters recorded in the case files and additional parameters of interest recorded as sequences are automatically loaded.There are many visualization and even secondary calculation options present that can be accessed on a Graphical User Interface (GUI) basis.
To observe cooling effect and vapor generation , contour plots of total temperature and vapor volume fraction are generated in all domains. As contour line density is increased and filled contour options are enabled , the color maps represent even the slightest variations with vivid detail.These contours can easily be animated using timestep animation generator.

To generate time evolution or two parameter correlation curves a probe point is to be selected where the parameter variation data would be collected from.Two probe points located at (0,-0.1,-0.002) and (0,0.1,-0.002) are considered as representatives of evaporator and condenser section.*CFD Post*® is not ideal for generating the curves from this probed data due to lesser flexibility. The data is hence exported as Comma Separated Values (CSV) for further processing.

8.2 MS EXCEL

Before plotting the data statistical processing is needed to ensure reliable data visualization.These data processing steps are performed using *MS Excel*®.
The data is filtered using regression strategy to look for potential outliers which are then removed.Proper rounding and decimal accuracy matching is also done.Finally a pivoted row sorting is done to make the plotting easy to interpret.

8.3 MATLAB

The final plotting is done using *Matlab*®.The processed CSV is imported as dataset from which columns are extracted as vectors.These are plotted under proper graphing configuration to match the scale and ensure better readability.
The aesthetic processing of the graph is done here as well due to versatility of the plot environment and presence of plot property manager.Generation and exporting of the graphs concluded the post-processing stage.

Part III

CONCLUSION

Visual representation and comparison of the simulation data along with author's analysis and prospective future recommendations.

9 RESULTS

In the present chapter the post-processed results are presented in a comprehensive manner to convey the complete simulation summary concisely.Principle focus is given to observe thermal performance but results on vaporization data are also analyzed with care in an attempt to describe the performance changes.

9.1 TEMPERATURE VARIATION

As the principle purpose of the heat-pipe is to act as a fast cooling device , temperature variations in zones of interest are carefully observed.Evaporator cooling performance and associated thermal loading in condenser section are considered as thermal performance deciding criteria.

9.1.1 *Cooling at Evaporator*

The evaporator cooling with nanofluid is higher than that of conventional water loaded ones as expected.Interestingly enough the curve shows an approximately exponential trend which suggests the system is of first order nature.

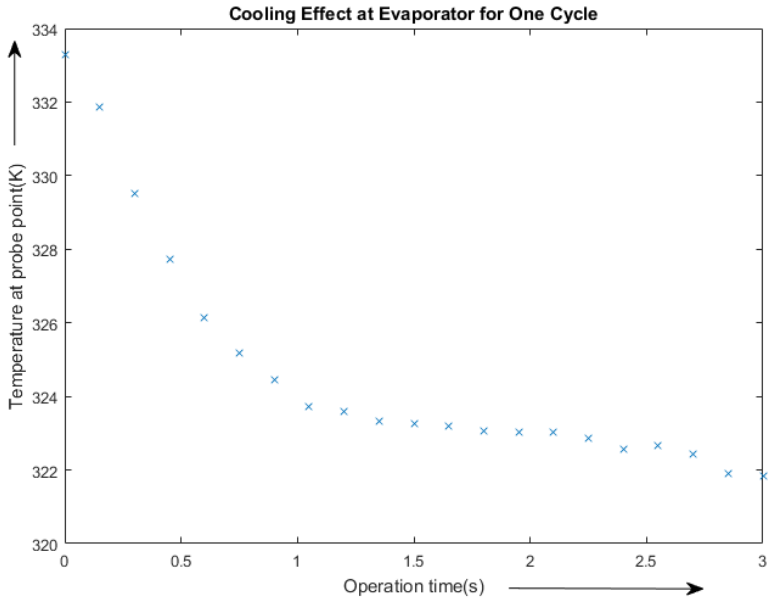

Figure 8: Evaporator cooling with nanofluid and inactive magnetic field

When the magnetic field is turned on initially the performance is found to be lower but eventually after a cut-point magnetohydrodynamic effects become significant and the cooling becomes faster.

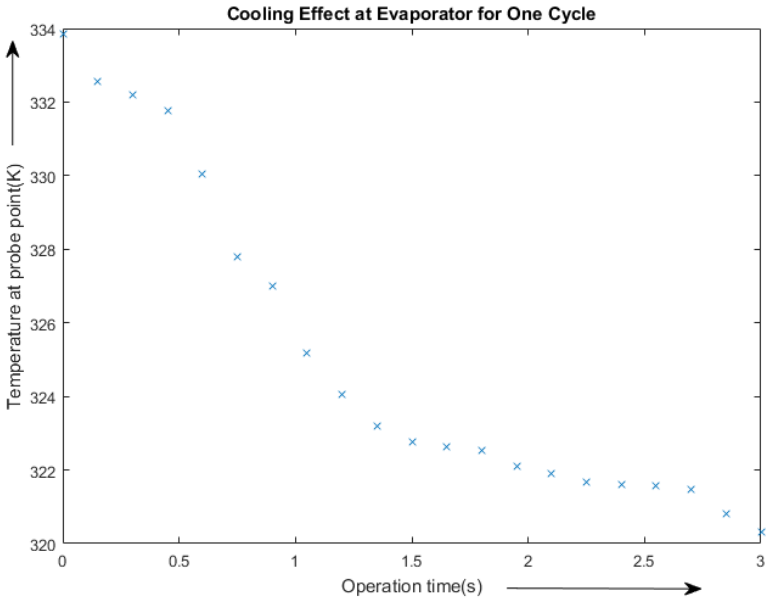

Figure 9: Evaporator cooling with nanofluid and active magnetic field

The lower performance in the beginning is due to opposite induction field in the ferrofluid due to Lenz law induction.The fluid flowfield undergoes a complex microscopic assortment before the cut point is reached.The additional pressure gradient created during this phase provides advective acceleration to the fluid once this point is passed.

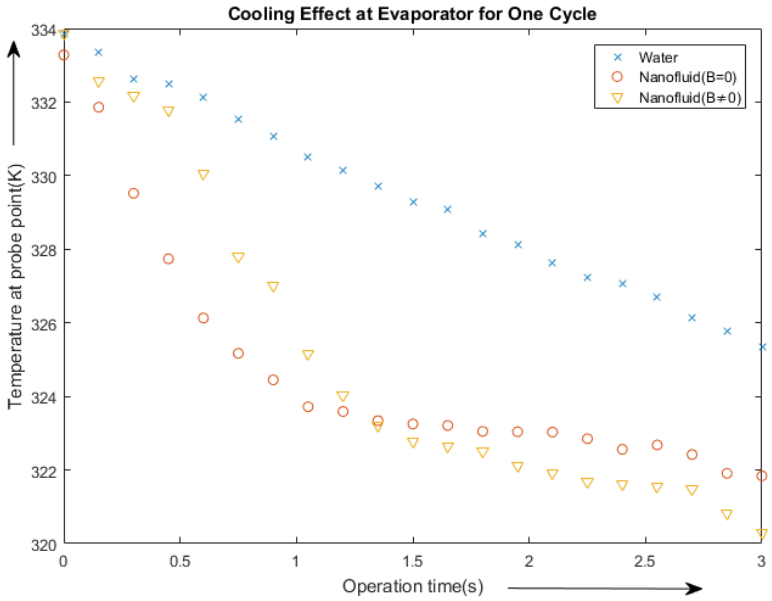

Figure 10: Evaporator cooling behavior comparison

The ferrofluid enhancement of the performance is obvious from the comparison plot.Effect of magnetic field seems very small in this interval but the effect grows with time as the thermomagnetic pumping potential is accumulated.
The skewness that the nanofluid curve experiences is due to agglomeration of nanoparticles during phase transition.The inflection is absent in case of water due to null agglomeration.

9.1.2 *Condenser Condition*

Due to different amount of heat flux absorption at the evaporator , the heat rejection and hence temperature levels at the condenser are directly affected.

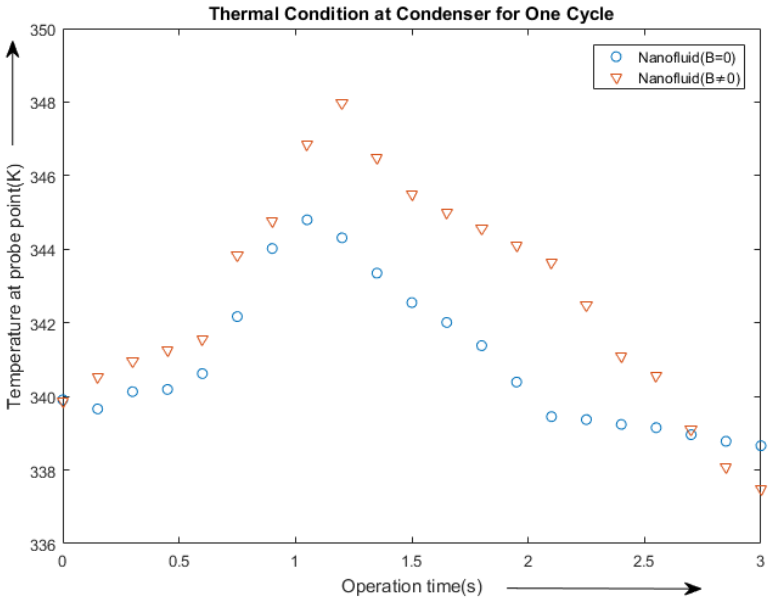

Figure 11: Condenser temperature variation comparison

As ferrofluid picks up more heat at the evaporator it rejects more heat at the condenser resulting in higher peak at condenser.This can be easily solved by incorporating a Pulse Width Modulation (PWM) control on the cooling fan. [1].The higher heat rejection would prove to e beneficial in the long run as it would cool the heat source faster providing a shorter overall response time.

9.2 VAPORIZATION PATTERN

The vaporization pattern is observed by generating timestep animation of the vapor volume fraction contour plots.Frames of such contours , setup chronologically , can provide great insight about the phase transition process.

As it can be seen the vapor progresses symmetrically through both parallel pipe segments.The process gets accelerated once the magnetic field makes the fluid pick up it's pace. Eventually the two vapor streams collide at the condenser and this reduces bulk motion which facilitates the condensation process.

9.3 HEAT TRANSFER CHARACTERISTICS

To compare heat transfer behavior Nu versus Re plots are generated.The plots span a small interval along Re axis as there is no separate pumping device present and all of the movement is due to density effects

1 PWM would automatically adjust airflow to keep peak temperature controlled

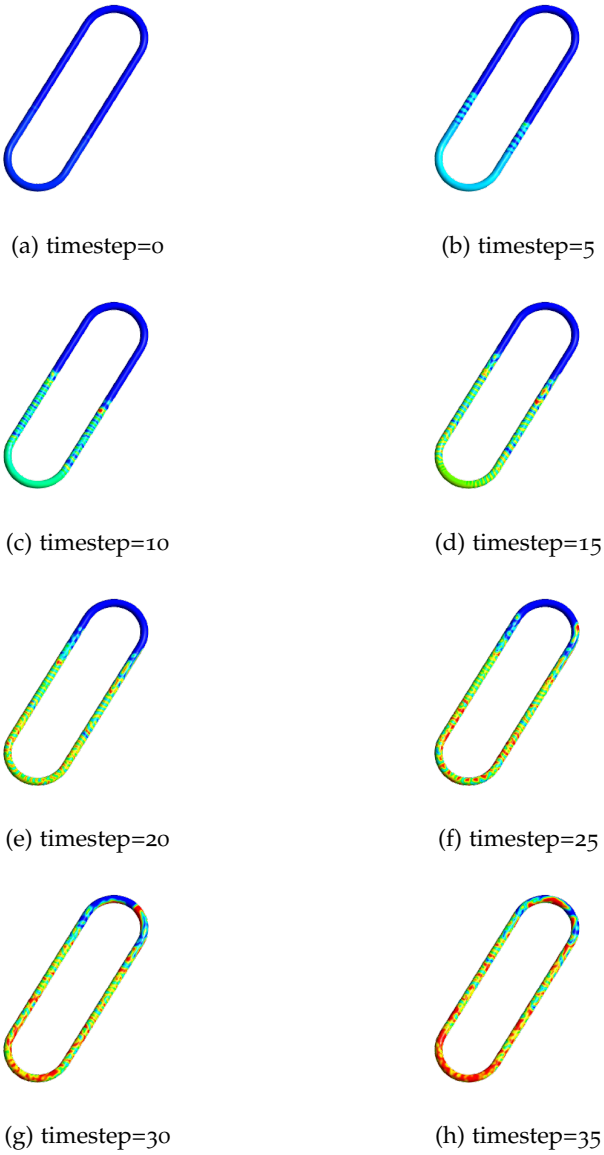

(a) timestep=0 (b) timestep=5

(c) timestep=10 (d) timestep=15

(e) timestep=20 (f) timestep=25

(g) timestep=30 (h) timestep=35

Figure 12: Evolution of vapor volume fraction

obtained via natural convection.The Nu ranges are pretty high as the value of convective heat transfer coefficient is improved due to enhanced thermal properties of the nanofluid.

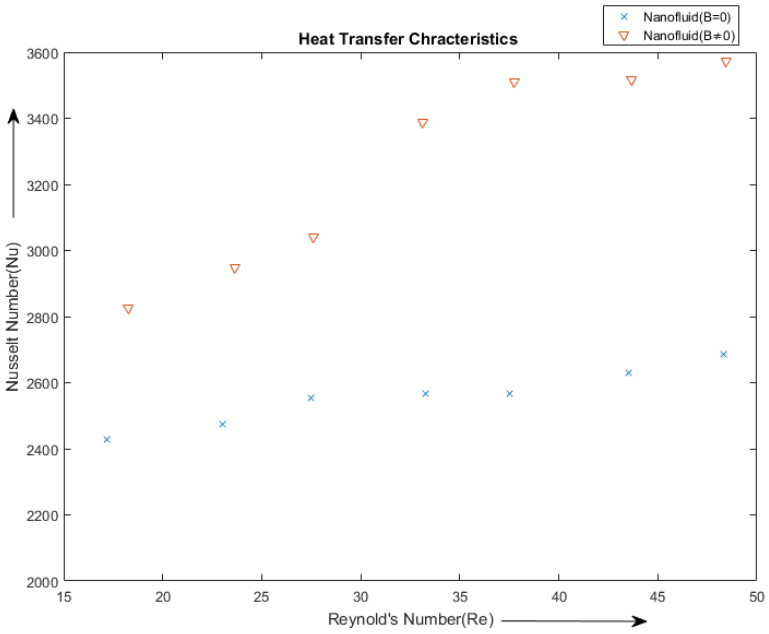

Figure 13: Heat transfer comparison

With magnetic field the values are higher due to-

- velocity boost resulting from thermomagnetic pumping
- thermal conductivity increment due to anisotropy reduction
- higher evaporation frequency due to multinucleation

The gap between active and inactive magnetic excitation increases with increasing Re due to additional vortex formation and magneto-hydrodynamic turbulence which increases heat transfer.

10 DISCUSSION

10.1 RESULT SUMMARY

The graphs and contour maps presented in Chapter 9 show some definite trends which can be summarized to make the concluding remarks on what this work has established.

Heat Removal Rate heat removal is faster when magnetic field is present as evident by the Nu vs Re plot.This could be attributed to thermal conductivity increment due to microscale motion.

Vapor Onset observation of volume fraction contours indicate more nucleation site formation in the liquid domain when magnetic field is present which creates a faster vapor onset.

Void Spread under magnetic field the void spread is quicker as observed in the evolution of the volume fraction of vapor contours.A possible reason for this could be the quicker vapor onset.

Velocity Field under magnetic field the velocity field is more vigorous and Re values are much higher.This is due to the negative viscosity effect mentioned by Schliomis[39].

Response Initiation for the case with active magnetive field the response is quicker but the response is initiated later compared to the inactive magnetic field case.This could be explained if induction effects are critically observed.A valid hypothesis is the initial induction field opposes the applied field due to Lenz's law which leads to reduced movement at the beginning , but this effect is easily outweighed by the thermomagnetic pumping later on.

10.2 LIMITATIONS

Although the simulations are handled quite rigorously , there are certain limitations imposed on the results due to modeling and solution assumptions.

- the ferrofluid magnetic induction is assumed to be independent of external field which is not true in reality due to hysteresis effects
- nanoparticle wall entrainment effects have not been considered
- nanoparticle exchange between incompressible liquid domain and compressible gas domain has not been properly modeled

- some property values are extrapolated or obtained via analogy due to lack of thermophysical data
- effect spheres around the nanoparticles are not separately treated with any special treatment

The limitations do change the results from what would be the real case but the overall trend should be expected as is found in the analysis presented hereto.

11

FUTURE RECOMMENDATION

- the current work has been performed with low number of total time-steps due to computational resource limitation . This can be extended in future.
- the study is computational and hence acts only as a model . Hence experimental validation could be done to test the legibility of the results.
- the study is performed under saturated magnetic field condition.It can be expanded by including other unsaturated conditions to observe field variation effects.
- the work can be extended to flatface and multiloop heat-pipes to compare relative advantage
- if possible a sintered wick case could be studied in quest of designing a non interfering wick structure while nanofluid is vaporized

Part IV

APPENDIX

A

MAGNETOHYDRODYNAMIC EFFECT:THERMOMAGNETIC PUMPING

Consider fluid flow under the following assumptions-

- incompressible flow
- steady state operation
- negligible viscous effect
- one dimensional flow
- null anisotropy of fluid properties
- homogeneous fluid domain

These assumptions make the flow idealized and simpler to model the phenomena.
To observe thermomagnetic pumping , fluid is assumed to be magnetically responsive and an external magnetic field aiding the flow is considered.

Continuity equation:

$$\vec{\nabla}(\rho\vec{V}) + \frac{\partial \rho}{\partial t} = 0$$
$$\implies \frac{\partial u}{\partial x} = 0$$
$$\implies u = f(y)$$

Momentum equation:

$$\rho\left(\frac{\partial \vec{V}}{\partial t} + (\vec{V}\cdot\vec{\nabla})\vec{V}\right) = -\vec{\nabla}P + \mu\nabla^2\vec{V} + \vec{f}$$
$$\implies \frac{\partial P}{\partial x} = \mu\frac{d^2u}{dy^2} + f$$
$$\implies \frac{\partial P}{\partial x} \approx f$$

Alfven[4] MHD Equation:

$$P_B = \frac{B^2}{2\widetilde{\mu}}$$

$$\implies f = \frac{\partial P_B}{\partial x} = \frac{B}{\widetilde{\mu}}\frac{\partial B}{\partial x}$$

Substituting f ,

$$\frac{\partial P}{\partial x} = \frac{B}{\widetilde{\mu}}\frac{\partial B}{\partial x}$$

$$\implies \int_{x_i}^{x_f} \frac{\partial P}{\partial x} dx = \frac{1}{\widetilde{\mu}} \int_{x_i}^{x_f} B \frac{\partial B}{\partial x} dx$$

$$P(x) = P_0 + \underbrace{\frac{1}{\widetilde{\mu}} \int_{x_i}^{x_f} B \frac{\partial B}{\partial x} dx}_{\text{MHD Pressure}}$$

This boost in pressure initiates thermomagnetic pumping effect.The equations are slightly complicated albeit similar in more realistic cases.

BIBLIOGRAPHY

[1] URL: https://antec.com/product/cooling/a400-rgb.php.

[2] *Acetone | CH3COCH3 - PubChem*. https://pubchem.ncbi.nlm.nih.gov/compound/Acetone.

[3] *Acetone*. https://webbook.nist.gov/cgi/cbook.cgi?ID=C67641&Mask=4.

[4] H.O.G. Alfven. "Cosmology in the plasma universe: an introductory exposition." In: *IEEE Transactions on Plasma Science* 18.1 (1990), pp. 5–10. DOI: 10.1109/27.45495. URL: https://doi.org/10.1109/27.45495.

[5] A. Bejan. *Convection Heat Transfer*. 3rd Edition. NY,USA: John Wiley, 2004.

[6] Hsin-Ping Chang, Hung-Chih Liu, and Chung-Sung Tan. "Using supercritical CO2-assisted mixing to prepare graphene/-carbon nanotube/epoxy nanocomposites." In: *Polymer* 75 (Sept. 2015), pp. 125–133. DOI: 10.1016/j.polymer.2015.08.023. URL: https://doi.org/10.1016/j.polymer.2015.08.023.

[7] Lifei Chen, Huaqing Xie, Yang Li, and Wei Yu. "Nanofluids containing carbon nanotubes treated by mechanochemical reaction." In: *Thermochimica Acta* 477.1-2 (Oct. 2008), pp. 21–24. DOI: 10.1016/j.tca.2008.08.001. URL: https://doi.org/10.1016/j.tca.2008.08.001.

[8] Anushree Chintaparthi and John Philip. "Assessment of Long term Stability of Aqueous Nanofluids Using Different Experimental Techniques." In: *Journal of Molecular Liquids* 222 (July 2016). DOI: 10.1016/j.molliq.2016.07.051.

[9] S U.S. Choi and J A Eastman. "Enhancing thermal conductivity of fluids with nanoparticles." In: *Agonne* (). URL: https://www.osti.gov/biblio/196525.

[10] *DOE spol. s r.o. – the distributor of electronic components*. https://www.doe.cz/en/.

[11] Leighton E. Sissom Donald R. Pitts. *Heat Transfer*. 1st Edition. McGraw Hill, 1977.

[12] J.A. Eastman, S.R. Phillpot, S.U.S. Choi, and P. Keblinski. "THERMAL TRANSPORT IN NANOFLUIDS." In: *Annual Review of Materials Research* 34.1 (2004), pp. 219–246. DOI: 10.1146/annurev.matsci.34.052803.090621. eprint: https://doi.org/10.1146/annurev.matsci.34.052803.090621. URL: https://doi.org/10.1146/annurev.matsci.34.052803.090621.

[13] Howell John Faghri Amir Zhang Yuwen. *Advanced Heat and Mass Transfer*. Columbia ,MO: Global Digital Press, 2010.

[14] M. Fakour, A. Vahabzadeh, and D.D. Ganji. "Study of heat transfer and flow of nanofluid in permeable channel in the presence of magnetic field." In: *Propulsion and Power Research* 4.1 (Mar. 2015), pp. 50–62. DOI: 10.1016/j.jppr.2015.02.005. URL: https://doi.org/10.1016/j.jppr.2015.02.005.

[15] *Gallica* -. http://visualiseur.bnf.fr/CadresFenetre?O=NUMM-3063&M=tdm.

[16] Ali Ghofrani, M.H. Dibaei, Abbas Hakim sima, and Mohammad Shafii. "Experimental investigation on laminar forced convection heat transfer of ferrofluids under an alternating magnetic field." In: *Experimental Thermal and Fluid Science* 49 (Sept. 2013), 193–200. DOI: 10.1016/j.expthermflusci.2013.04.018.

[17] Hamid Goshayeshi, Mohammad Reza Safaei, Marjan Goodarzi, and Mahidzal Dahari. "Particle size and type effects on heat transfer enhancement of Ferro-nanofluids in a pulsating heat pipe." In: *Powder Technology* 301 (Aug. 2016). DOI: 10.1016/j.powtec.2016.08.007.

[18] F. Polasek H. Akachi and P. Stulc. "Pulsating heat pipes." In: *5th International Heat Pipe Symposium* (1996), 208–217.

[19] R. L. Hamilton and O. K. Crosser. "Thermal Conductivity of Heterogeneous Two-Component Systems." In: *Industrial & Engineering Chemistry Fundamentals* 1.3 (Aug. 1962), pp. 187–191. DOI: 10.1021/i160003a005. URL: https://doi.org/10.1021/i160003a005.

[20] *Heat Pipe Technology, Working Priniciples, Wick Structures, Performance*. https://celsiainc.com/technology/heat-pipe/.

[21] Chungpyo Hong, Yutaka Asako, and Jae-Heon Lee. "Heat transfer characteristics of gaseous flows in micro-channel with constant heat flux." In: *International Journal of Thermal Sciences* 46.11 (Nov. 2007), pp. 1153–1162. DOI: 10.1016/j.ijthermalsci.2006.10.015. URL: https://doi.org/10.1016/j.ijthermalsci.2006.10.015.

[22] Nathan Hordy, Delphine Rabilloud, Jean-Luc Meunier, and Sylvain Coulombe. "High temperature and long-term stability of carbon nanotube nanofluids for direct absorption solar thermal collectors." In: *Solar Energy* 105 (July 2014), 82–90. DOI: 10.1016/j.solener.2014.03.013.

[23] Mohammed Noorul Hussain and Isam Janajreh. "Numerical simulation of a cylindrical heat pipe and performance study." In: *International Jouranl of Thermal & Environmental Engineering* 12.2 (2016), pp. 135–141.

[24] Y. Hwang, J.K. Lee, C.H. Lee, Y.M. Jung, S.I. Cheong, C.G. Lee, B.C. Ku, and S.P. Jang. "Stability and thermal conductivity characteristics of nanofluids." In: *Thermochimica Acta* 455.1-2 (Apr. 2007), pp. 70–74. DOI: 10.1016/j.tca.2006.11.036. URL: https://doi.org/10.1016/j.tca.2006.11.036.

[25] Shung-Wen Kang, Wei-Chiang Wei, Sheng-Hong Tsai, and Chia-Ching Huang. "Experimental investigation of nanofluids on sintered heat pipe thermal performance." In: *Applied Thermal Engineering* 29.5-6 (Apr. 2009), pp. 973–979. DOI: 10.1016/j.applthermaleng.2008.05.010. URL: https://doi.org/10.1016/j.applthermaleng.2008.05.010.

[26] Keqin Li. "Power and performance management for parallel computations in clouds and data centers." In: *Journal of Computer and System Sciences* 82.2 (Mar. 2016), pp. 174–190. DOI: 10.1016/j.jcss.2015.07.001. URL: https://doi.org/10.1016/j.jcss.2015.07.001.

[27] H. B. Ma, M. A. Hanlon, and C. L. Chen. "An investigation of oscillating motions in a miniature pulsating heat pipe." In: *Microfluidics and Nanofluidics* 2.2 (Dec. 2005), pp. 171–179. DOI: 10.1007/s10404-005-0061-8. URL: https://doi.org/10.1007/s10404-005-0061-8.

[28] Sidi Maïga, Samy Palm, Cong Nguyen, Gilles Roy, and Nicolas Galanis. "Heat transfer enhancement by using nanofluids in forced convection flows." In: *International Journal of Heat and Fluid Flow,Elsevier(SCOPUS Indexed)* 26 (Aug. 2005), pp. 530–546. DOI: 10.1016/j.ijheatfluidflow.2005.02.004.

[29] Mohammad Mehrali, Emad Sadeghinezhad, Reza Azizian, Amir Akhiani, Sara Tahan Latibari, Mehdi Mehrali, and Hendrik Metselaar. "Effect of nitrogen-doped graphene nanofluid on the thermal performance of the grooved copper heat pipe." In: *Energy Conversion and Management* 118 (June 2016), pp. 459–473. DOI: 10.1016/j.enconman.2016.04.028.

[30] Daisie D. Boettner Margaret B. Bailey Michael J. Moran Howard N. Shapiro. *Fundamentals of Engineering Thermodynamics*. 7th Edition. Wiley.

[31] S. Valiallah Mousavi, M. Barzegar Gerdroodbary, Mohsen Sheikholeslami, and D. D. Ganji. "The influence of a magnetic field on the heat transfer of a magnetic nanofluid in a sinusoidal channel." In: *The European Physical Journal Plus* 131.9 (Sept. 2016). DOI: 10.1140/epjp/i2016-16347-4. URL: https://doi.org/10.1140/epjp/i2016-16347-4.

[32] Henry Petroski. *To Engineer is Human:The Role of Failure in Success*. 1st Edition. 5th Avenue, NY, USA: McMillan Publishers, 1985.

[33] Amin Puia, Roghayeh Ghasempour, Mohammad Ahmadi, Gholamreza Heydarian, and Mohammad Shafii. "Experimental investigation of graphene oxide nanofluid on heat transfer enhancement of pulsating heat pipe." In: *International Communications in Heat and Mass Transfer* 91 (Feb. 2018), pp. 90–94. DOI: 10.1016/j.icheatmasstransfer.2017.12.006.

[34] Mayur Shrikhande Pulkit Agarwal and P. Srinivasan. "Heat Transfer Simulation by CFD from Fins of an Air Cooled Motorcycle Engine under Varying Climatic Conditions." In: *The World Congress on Engineering 2011 Volume-3 WCE 2011* (2011).

[35] *Safe CPU Temps: How Hot Should My CPU Be? (Idle & Under Load)*. https://techguided.com/safe-cpu-temp/.

[36] Amin Shahsavar, Mohammad Reza Salimpour, Mohsen Saghafian, and M. B. Shafii. "Effect of magnetic field on thermal conductivity and viscosity of a magnetic nanofluid loaded with carbon nanotubes." In: *Journal of Mechanical Science and Technology* 30.2 (Feb. 2016), pp. 809–815. DOI: 10.1007/s12206-016-0135-4. URL: https://doi.org/10.1007/s12206-016-0135-4.

[37] M. Sheikholeslami, M. Jafaryar, Dr. Salman Saleem, Zhixiong Li, Ahmad Shafee, and Yu Jian. "Nanofluid heat transfer augmentation and exergy loss inside a pipe equipped with innovative turbulators." In: *International Journal of Heat and Mass Transfer* 126 (May 2018). DOI: 10.1016/j.ijheatmasstransfer.2018.05.128.

[38] Weixiu Shi and Lisheng Pan. "Influence of filling ratio and working fluid thermal properties on starting up and heat transferring performance of closed loop plate oscillating heat pipe with parallel channels." In: *Journal of Thermal Science* 26.1 (Jan. 2017), pp. 73–81. DOI: 10.1007/s11630-017-0912-0. URL: https://doi.org/10.1007/s11630-017-0912-0.

[39] Mark I. Shliomis and Konstantin I. Morozov. "Negative viscosity of ferrofluid under alternating magnetic field." In: *Physics of Fluids* 6.8 (Aug. 1994), pp. 2855–2861. DOI: 10.1063/1.868108. URL: https://doi.org/10.1063/1.868108.

[40] C C Silverstein. *Design and Technology of Heat Pipes for Cooling and Heat Exchange*. 1st Edition. United States, 1992.

[41] Dawid Taler. "Simple power-type heat transfer correlations for turbulent pipe flow in tubes." In: *Journal of Thermal Science* 26.4 (2017), pp. 339–348.

[42] Erjun Tang, Guoxiang Cheng, Xiaolu Ma, Xingshou Pang, and Qiang Zhao. "Surface modification of zinc oxide nanoparticle by PMAA and its dispersion in aqueous system." In: *Applied Surface Science* 252.14 (May 2006), pp. 5227–5232. DOI: 10.1016/

j.apsusc.2005.08.004. URL: https://doi.org/10.1016/j.apsusc.2005.08.004.

[43] Md. Riyad Tanshen, M.J. Munkhbayar, H. Nine, and H. Jeong. "Effect of functionalized MWCNTs/water nanofluids on thermal resistance and pressure fluctuation characteristics in oscillating heat pipe." In: *Int Commun Heat Mass* 48 (Jan. 2013), pp. 93–98.

[44] *Testing Thermal Throttling in Pentium 4 CPUs with Northwood and Prescott cores*. http://ixbtlabs.com/articles2/p4-throttling/.

[45] Trijo Tharayil, Lazarus Godson Asirvatham, Vysakh Ravindran, and Somchai Wongwises. "Effect of filling ratio on the performance of a novel miniature loop heat pipe having different diameter transport lines." In: *Applied Thermal Engineering* 106 (Aug. 2016), pp. 588–600. DOI: 10.1016/j.applthermaleng.2016.05.125. URL: https://doi.org/10.1016/j.applthermaleng.2016.05.125.

[46] *The International Association for the Properties of Water and Steam*. URL: http://www.iapws.org/relguide/Surf-H2O-2014.pdf.

[47] Eman Tora and Tarek Moustafa. "Numerical Simulation of an Al2O3-H2O Nanofluid as a Heat Transfer Agent for a Flat-Plate Solar Collector." In: *International Journal of Scientific Engineering Research* 4 (May 2013), pp. 762–773.

[48] Huaqing Xie, Jinchang Wang, Tonggeng Xi, Yan Liu, Fei Ai, and Qingren Wu. "Thermal Conductivity Enhancement of Suspensions Containing Nanosized Alumina Particles." In: *Journal of Applied Physics* 91 (Apr. 2002), pp. 4568–4572. DOI: 10.1063/1.1454184.

[49] Xuefei Yang and Zhen hua Liu. "A Kind of Nanofluid Consisting of Surface-Functionalized Nanoparticles." In: *Nanoscale Research Letters* 5.8 (May 2010), pp. 1324–1328. DOI: 10.1007/s11671-010-9646-6. URL: https://doi.org/10.1007/s11671-010-9646-6.

[50] *https://ferrofluid.ferrotec.com/products/ferrofluid-audio/apg-e/apg-e32/*. https://ferrofluid.ferrotec.com/products/ferrofluid-audio/apg-e/apg-e32/. (Accessed on 02/03/2020).